Available online at www.sciencedirect.com
ScienceDirect
Electric Power Systems Research 78 (2008) 337–345
ELECTRIC POWER SYSTEMS RESEARCH
www.elsevier.com/locate/epsr

Improving large-disturbance stability through optimal bifurcation control and time domain simulations

Wei Gu [a,*], Federico Milano [b], Ping Jiang [a], Jianyong Zheng [a]

[a] SouthEast University, School of Electrical Engineering, NanJing, China
[b] University of Castilla-La Mancha, Department of Electrical Engineering, Ciudad Real 13071, Spain

Received 20 July 2006; received in revised form 17 January 2007; accepted 2 March 2007
Available online 11 April 2007

Abstract

This paper presents an approach for improving, through practical assumptions, the stability of power systems subjected to large disturbances. The proposed method is composed of two steps, solved iteratively. The first step solves an optimal bifurcation control problem that guarantees the small-signal stability of the equilibrium point. The proposed optimal bifurcation control addresses saddle-node and Hopf bifurcations. The second step is an $N-1$ contingency analysis computed through time domain simulations. The second step guarantees the large-disturbance stability of the equilibrium point. The WSCC 9-bus and New England 39-bus systems are used to illustrate and test the proposed technique.

Keywords: Optimal bifurcation control; Small-signal stability analysis; Large disturbance; $N-1$ contingency analysis; Saddle-node bifurcation; Hopf bifurcation

1. Introduction

Transient stability, or more in general, large-disturbance stability has always been a key topic of power system analysis [1–6]. However, there are still several issues, ranging from stability analysis methods to control schemes, that need to be addressed. Nowadays research studies face mainly two bottlenecks. (i) A huge amount of calculations, especially time domain simulations, is needed for large-disturbance stability studies. New generation computers and parallel processing can help in speeding up calculations. (ii) It is mathematically challenging to determine the stability region of a set of non-linear differential algebraic equations such as the power system model [3]. This paper addresses the latter point.

Time domain simulation (TDS) and energy function (EF) methods are the traditional approaches to study large-disturbance stability [3,4]. Some new results about TDS and EF methods can be found in Refs. [7,8], respectively. The TDS approach can be applied to any level of detail of power system models and gives a visual information about state variables. One of the main disadvantages of the TDS approach, except for being time-consuming, is that it does not provide information about the stability margin of the system. Therefore, the TDS approach is not effective for stability control. On the contrary, the EF approach is able to provide an index that measures the system stability. However, EF methods can be applied only to power system for which the energy function is known and only work for first-swing stability analysis. Due to these limitations, EF methods are typically used in conjunction with TDS methods [9,10]. In this vein, in this paper, the TDS analysis is used in conjunction with a small-signal stability constrained optimization problem.

Small-signal stability analysis techniques, based on bifurcation theory, has been proposed in Refs. [11–13]. The "feasibility region" or, in other words, the small-signal stability region, was presented in Ref. [12] to identify the stability region in the parameter space. This paper uses this concept of small-signal stability region for the formulation of an optimization problem. In particular, this paper addresses saddle-node and Hopf bifurcations.

The proposed optimization problem is based on a variety of stability constrained OPF problems that have been presented in the literature, such as the maximization of the distance to

* Corresponding authors. Tel.: +86 13814005169
E-mail addresses: WGu@seu.edu.cn (W. Gu), Federico.Milano@uclm.es (F. Milano).

0378-7796/$ – see front matter © 2007 Elsevier B.V. All rights reserved.
doi:10.1016/j.epsr.2007.03.002

voltage collapse [14–17]. The computation of the maximum loading condition is only a part of the information that can be used for avoiding instability. One can be interested in determining how control variables affect the loading margin [18]. Clearly this is useful both to determine the most critical variables and to design an effective corrective action to avoid the collapse [19]. This paper proposes an optimization problem that allows finding the critical stability condition of a power system.

It has to be noted the relevance of the variations of control parameters and their sensitivities with respect to the stability margin in several practical applications. For example, in Refs. [17,20,21], the stability region for the most critical contingency is determined through a sensitivity analysis, while in Refs. [22,23] parameter sensitivities are used to properly set up primary and secondary voltage regulation, respectively. In Ref. [24], voltage and transmission line thermal limits are used to determine the feasibility region of inter area power transfers.

Based on these results, this paper proposes an optimization problem to find the optimal control variable profile that ensures an adequate stability region with inclusion of an $N-1$ contingency criterion.

The optimization problem proposed in this paper is able to optimize system control parameters in order to ensure an adequate stability margin of the optimal equilibrium point. However, large-disturbance stability cannot be taken into account by the optimization problem. It is well known that dynamic bifurcations can be triggered by large-disturbances [25,26]. In Refs. [27,28], $N-1$ contingency analysis is obtained through extensive time domain simulations. In this vein, this paper proposes an iterative technique that combines the stability constrained optimization problem and simulation-based $N-1$ contingency analysis. The proposed iterative method leads to the definition of a control parameter set that guarantee both small and large-disturbance stability.

In summary the novel contribution of the paper are as follows:

(1) Proposal of a stability constrained OPF for optimizing control parameters. The solution of this OPF problem ensures the small-signal stability of the system. Stability constraints take into account saddle-node and Hopf bifurcations.
(2) Proposal of an iterative method that computes repeatedly the OPF problem and time domain simulations following contingencies. The result of this procedure is an equilibrium point that is stable for both small-signal stability and large-disturbance stability.

The paper is organized as follows. Section 2 provides outlines of differential-algebraic equations of power systems, bifurcation analysis and the definition of small-signal stability region. Section 3 presents the proposed optimal bifurcation control model and Section 4 presents the approach for taking into account $N-1$ contingency analysis and improving large-disturbances stability. In Section 5, the proposed technique is illustrated and tested through the WSCC 9-bus and the New England 39-bus test systems. Finally, in Section 6, conclusions are duly drawn.

2. Outlines of power system stability analysis

2.1. Differential algebraic equations

Power electric systems can be represented as a set of differential algebraic equations (DAE) [29]:

$$\dot{x} = f(x, y, \mu, p), \qquad 0 = g(x, y, \mu, p) \tag{1}$$

where ($f : \mathbb{R}^n \times \mathbb{R}^m \times \mathbb{R}^k \times \mathbb{R}^l \to \mathbb{R}^n$) is the vector of differential equations; $x \in \mathbb{R}^n$ the vector of state variables associated with generators, loads and system controllers; ($g : \mathbb{R}^n \times \mathbb{R}^m \times \mathbb{R}^k \to \mathbb{R}^m$) the vector of algebraic equations; $y \in \mathbb{R}^m$ the vector of algebraic variables; $\mu \in \mathbb{R}^k$ the vector of uncontrollable variables; and $p \in \mathbb{R}^l$ is the vector of control variables. It is assumed that algebraic variables can vary instantaneously, i.e. their transients are assumed to be "infinitely" fast.

Eq. (1) can be linearized at an equilibrium point (x_0, y_0, μ_0, p_0), as follows:

$$\begin{bmatrix} \Delta\dot{x} \\ 0 \end{bmatrix} = \begin{bmatrix} f_x & f_y \\ g_x & g_y \end{bmatrix} \begin{bmatrix} \Delta x \\ \Delta y \end{bmatrix} = A_{\text{tot}} \begin{bmatrix} \Delta x \\ \Delta y \end{bmatrix} \tag{2}$$

where A_{tot} is the full system Jacobian matrix, and $f_x = \partial f/\partial x|_0$, $f_y = \partial f/\partial y|_0$, $g_x = \partial g/\partial x|_0$ and $g_y = \partial g/\partial y|_0$ are the Jacobian matrices of the differential and algebraic equations with respect to the state and algebraic variables, respectively. If it is assumed that g_y is non-singular, the vector of algebraic variables Δy can be eliminated from Eq. (2), as follows:

$$\Delta\dot{x} = (f_x - f_y g_y^{-1} g_x)\Delta x = A_{\text{sys}}\Delta x \tag{3}$$

Thus the DAE can be implicitly reduced to a set of ordinary differential equations (ODE). Observe that if g_y is singular, the model of the system has to be revised as the dynamics of some algebraic equations cannot be neglected [30]. Thus it is always possible to formulate a set of DAE for which g_y is not singular.

In order to give a rigorous definition of the bifurcations discussed in this paper, let us assume that the uncontrollable variables are scalar, i.e. $\mu \in \mathbb{R}$. In our formulation, μ is the loading factor that multiplies load powers as follows:

$$P_{\text{L}}^{\mu} = \mu P_{\text{L}}^{0}, \qquad Q_{\text{L}}^{\mu} = \mu Q_{\text{L}}^{0} \tag{4}$$

where P_{L}^{0} and Q_{L}^{0} are the base case or initial load profile ($\mu = 1$ at the base case).

The loading factor is commonly used in stability studies to determine the maximum loading condition that can be either associated with Refs. [25,26,30]:

(1) voltage stability limit (collapse point) corresponding to a system singularity (saddle-node bifurcation);
(2) system controller limits such as generator reactive power limits (limit-induced bifurcation);
(3) frequency stability (Hopf bifurcation).

2.2. Bifurcations analysis

In this paper, bifurcation points are identified through the eigenvalue loci of the state matrix A_{sys}.

For the sake of definition, let us define the vector of functions F as follows:

$$\dot{x} = F(x, \mu) = f(x, y(x, \mu), \mu) \tag{5}$$

i.e. F is the set of differential equations where the algebraic variables y have been substituted for their explicit function of x and μ. Thus, one has:

$$A_{\text{sys}} = \frac{\partial F}{\partial x|_0} \tag{6}$$

Observe that, from the practical point of view, it is not necessary to know explicitly the function $y(x, \mu)$ since the state matrix A_{sys} can be computed from Eq. (3).

The bifurcations discussed in this paper are the saddle-node bifurcation and the Hopf bifurcation. The definitions of these bifurcations are as follows [11].

2.2.1. Saddle-node bifurcation (SNB)

A SNB point is an equilibrium point (x_0, μ_0) at which the state matrix presents one zero eigenvalue. SNB are associated with a pair of equilibrium points, one stable (s.e.p.) and one unstable (u.e.p.) that coalesce and disappear. The following transversality conditions hold:

(1) the state matrix A_{sys} has a simple and unique eigenvalue with right and left eigenvectors v and w such that $A_{\text{sys}}v = A_{\text{sys}}^{\text{T}}w = 0$;
(2) $w^{\text{T}}\partial F/\partial\mu|_0 = 0$;
(3) $w^{\text{T}}[\partial^2 F/\partial x^2]v \neq 0$.

2.2.2. Hopf bifurcation (HB)

A HB point is an equilibrium point (x_0, μ_0) at which the state matrix presents a complex conjugate pair of eigenvalues with zero real part. The following transversality conditions hold:

(1) the state matrix A_{sys} has a simple pair of purely imaginary eigenvalues $\lambda(\mu_0) = \pm j\beta$ and no other eigenvalues with zero real part;
(2) $\mathrm{d}\Re\{\lambda(\mu)/\mathrm{d}\mu|_0\} \neq 0$.

The HB gives a birth to a zero-amplitude limit cycle with initial period $T_0 = 2\pi/\beta$. If the limit cycle is stable the HB is "supercritical"; if the limit cycle is unstable the HB is "subcritical".

Observe that limit-induced bifurcations (LIBs) [30] are not discussed since, control limits of AVRs and of other system regulators are implicitly taken into account in the optimization problem that is proposed in Section 3.

2.3. Direct method for bifurcation analysis

The following direct method can be used to identify both SNB and HB [26]. Let us define $\lambda = \alpha + j\beta$ and u_x as one eigenvalue and its associated right eigenvector, respectively, of the matrix A_{sys}. Then:

$$A_{\text{sys}}u_x = \lambda u_x \tag{7}$$

Let us also define $u = [\,u_x^{\text{T}} \quad u_y^{\text{T}}\,]^{\text{T}}$, where $u_y = -g_y^{-1}g_x u_x$, thus Eq. (7) can be rewritten as:

$$\begin{bmatrix} f_x & f_y \\ g_x & g_y \end{bmatrix} \begin{bmatrix} u_x \\ u_y \end{bmatrix} = (\alpha + j\beta) \begin{bmatrix} u_x \\ 0 \end{bmatrix} \tag{8}$$

where

$$u_x = u_{x\text{R}} + ju_{x\text{I}}, \qquad u_y = u_{y\text{R}} + ju_{y\text{I}} \tag{9}$$

where $u_{x\text{R}}, u_{x\text{I}} \in \mathbb{R}^n$ and $u_{y\text{R}}, u_{y\text{I}} \in \mathbb{R}^m$. By substituting Eq. (9) in Eq. (8), one has:

$$\begin{aligned} 0 &= f_x u_{x\text{R}} + f_y u_{y\text{R}} - \alpha u_{x\text{R}} + \beta u_{x\text{I}}, \\ 0 &= f_x u_{x\text{I}} + f_y u_{y\text{I}} - \alpha u_{x\text{I}} - \beta u_{x\text{R}}, \qquad 0 = g_x u_{x\text{R}} + g_y u_{y\text{R}}, \\ 0 &= g_x u_{x\text{I}} + g_y u_{y\text{I}} \end{aligned} \tag{10}$$

Finally, considering the system DAE, Eq. (10) and imposing a non-trivial for the eigenvectors, one obtains the following set of equations:

$$\begin{aligned} 0 &= f(x, y, \mu, p), \qquad 0 = g(x, y, \mu, p), \\ 0 &= f_x u_{x\text{R}} + f_y u_{y\text{R}} - \alpha u_{x\text{R}} + \beta u_{x\text{I}}, \\ 0 &= f_x u_{x\text{I}} + f_y u_{y\text{I}} - \alpha u_{x\text{I}} - \beta u_{x\text{R}}, \qquad 0 = g_x u_{x\text{R}} + g_y u_{y\text{R}}, \\ 0 &= g_x u_{x\text{I}} + g_y u_{y\text{I}}, \qquad 1 = u_{x\text{R}}^{\text{T}} u_{x\text{R}} - u_{x\text{I}}^{\text{T}} u_{x\text{I}}, \\ 0 &= u_{x\text{R}}^{\text{T}} u_{x\text{I}} - u_{x\text{I}}^{\text{T}} u_{x\text{R}} \end{aligned} \tag{11}$$

Observe that Eq. (11) is valid for both SNB and HB points, as follows:

- at SNB points, $u_{x\text{R}} = u_x$, $u_{y\text{R}} = u_y$, $u_{x\text{I}} = u_{y\text{I}} = 0$, and $\alpha = \beta = 0$;
- at HB points, $\alpha = 0$ and $\beta \neq 0$.

Observe also that Eq. (11) is seldom used for computing bifurcation points because obtaining a solution highly depends on a good initial guess of the eigenvectors [30]. However this formulation is useful if used within an optimization problem, as discussed in Section 3.

2.4. Stability manifold

A definition of "small signal stability region", say Ω_{SSSR}, also called "feasibility region", was given in Refs. [12,13]. According to that definition, Ω_{SSSR} is "the stability region in the variable space, which is composed of all equilibrium points that can be reached quasi-statically from the current operating point without loss of local stability". If singularity-induced bifurcations are not a concern (i.e. g_y is non-singular), the small-signal stability region can be rewritten as $\Omega_{\text{SSSR}} = \{\overline{B_{\text{SNB}} \cup B_{\text{HB}} \cup B_{\text{LIB}}}\}$, where B_{SNB} is the unstable region identified by SNB points, B_{HB} the unstable region identified by HB points, and B_{LIB} is the unstable region identified by LIB points.

Observe that there is no general technique to obtain the entire stability region of a set of DAE, except for solving several computationally expensive time domain simulations with negative

time [11]. Furthermore, time domain techniques are effective only for a reduced number of state variables x and control variables p.

3. Optimal bifurcation control

The optimal bifurcation control (OBC) can be defined as the optimal configuration of control variables p so that the solution is within the small-signal stability region Ω_{SSSR}. In the OBC analysis, one has to minimize a control "cost" that is a function of control variables.

The OBC approach proposed in this paper is a non-linear optimization problem, as follows:

$$
\begin{aligned}
&\text{Min. } C(p)\\
&\text{s.t. } \quad 0 = f(x, y, \mu, p)\\
&\qquad 0 = g(x, y, \mu, p)\\
&\qquad 0 = f_x u_{x\mathrm{R}} + f_y u_{y\mathrm{R}} + \beta u_{x\mathrm{I}}\\
&\qquad 0 = f_x u_{x\mathrm{I}} + f_y u_{y\mathrm{I}} - \beta u_{x\mathrm{R}}\\
&\qquad 0 = g_x u_{x\mathrm{R}} + g_y u_{y\mathrm{R}}\\
&\qquad 0 = g_x u_{x\mathrm{I}} + g_y u_{y\mathrm{I}}\\
&\qquad 1 = u_{x\mathrm{R}}^{\mathrm{T}} u_{x\mathrm{R}} - u_{x\mathrm{I}}^{\mathrm{T}} u_{x\mathrm{I}}\\
&\qquad 0 = u_{x\mathrm{R}}^{\mathrm{T}} u_{x\mathrm{I}} - u_{x\mathrm{I}}^{\mathrm{T}} u_{x\mathrm{R}}\\
&\qquad \mu \geq \mu^{\min}\\
&\qquad h(x, y, \mu, p) \leq 0
\end{aligned}
\tag{12}
$$

where $C(p)$ is the objective function that represents the "cost" of changing control variables p. In this paper the following structure will be used:

$$
C(p) = \sum_i c_i (p_i - p_i^0)^2 \tag{13}
$$

where p_i^0 and c_i are the standard or default value and the weight, respectively, of the control variable p_i. The inequalities $h (h \in \mathbb{R}^{\ell})$ represent physical and security constraints such as voltage limits, regulators limits, etc.

The loading factor constraint $\mu \geq \mu^{\min}$ imposes that the solution has to present a minimum loading level. If $\mu > 1$, the system can be overloaded with respect to the base case. Observe that increasing $\mu^{\min}$ typically leads to increase the objective function.

For a given minimum value of the loading factor $\mu^{\min}$, the solution of Eq. (12) provides the bifurcation point that minimizes the control variable variation. Observe that the proposed model is able to find both SNB and HB points. LIB points are also taken implicitly into account through inequalities h.

Observe that changing regulator gains and/or other controller parameters p can highly impact the overall system stability. At this aim, Eq. (12) takes into account the differential-algebraic equations f and g of the system. Differential equations f include machine models and regulator control loops. Thus the solution of Eq. (12) ensures the local stability of the dynamic system at the optimal equilibrium point.

Observe also that Eq. (12) guarantees the *best* set of control parameters p only for local stability. This is because the contingency analysis is not directly included in Eq. (12). There is currently no well-assessed and efficient method that allows including large-disturbance stability constraints (which basically implies the use of time domain simulations) in an OPF problem.

In this paper the inclusion of contingencies is obtained through an iterative method that is described in Section 4.

4. $N-1$ contingency analysis

The solution of Eq. (12) is within the small-signal stability region as defined in Ref. [12]. However, it is possible that a contingency (e.g. a line outage) triggers a bifurcation. It is thus necessary to take into account an $N-1$ contingency analysis.

We make the following practical assumptions to guarantee the large-disturbance stability and, in turn, to include the $N-1$ contingency analysis in the optimal bifurcation control:

(1) The post-contingency large-disturbance stability region in the variable space is a subset of the small-signal stability region under the same contingency. This is a conservative assumption.
(2) The lower the loading margin, the higher the stability margin of the system. Thus it is always possible to find a post-disturbance stable condition. This assumption can be easily proved since a system with no load and with no generation ($\mu = 0$) is certainly stable.
(3) The sensitivity of the loading factor with respect to a control variable, say $\mathrm{d}\mu/\mathrm{d}p$, at a solution point maintains its sign after the occurrence of a large perturbation. This assumption is not true in general, however it holds for a variety of typical control variables and can thus be used to approximate the large-disturbance stability based on the small-signal stability region.

In our approach, the uncontrollable variable μ is used to define the frontier of the stability region Ω_{SSSR}, as follows. If the system shows a bifurcation point for a given value of the loading factor $\mu = \mu^{\mathrm{crit}}$, then all the equilibrium points are stable for $\mu < \mu^{\mathrm{crit}}$. We assume that if μ^{crit} is sufficiently high, and thus the small-signal stability region Ω_{SSSR} sufficiently big, then the system is also stable for large disturbances.

Problem (12) is then used to find the optimal profile of the control variables p that leads to the desired stability margin (i.e. $\mu \geq \mu^{\min}$) for a given contingency. However, since Eq. (12) only guarantees a local stability, one has to check that the system is stable for a large perturbation (e.g. line outages) by means of time domain simulations. If the system is not stable, one has to increase the stability margin $\mu^{\min}$, thus increasing Ω_{SSSR}.

It is relevant to note that the use of time domain simulations also allows excluding the occurrence of transient instabilities. Thus the proposed technique is also suitable for transient stability control.

This approach can be summarized as follows:

(1) Initialization of the stability margin $\mu_0^{\min} = 1$. This step imposes that the base case solution is feasible and stable.

(2) The base case solution undergoes a contingency ranking technique. One line outage is considered at a time and the stability of the post-contingency equilibrium is evaluated. The contingency that leads to the minimum value of μ is considered the worst contingency. If no contingency produces bifurcations go to step (5), otherwise go to step (3).
(3) Set $\mu^{\min}_{(n+1)} = \mu^{\min}_{(n)} + \Delta$, where Δ is a given increment of the stability margin. This step imposes that the base case solution has a stability margin $\mu^{\min} > 1$, thus enlarging the stability region of the system.
(4) Solve Eq. (12). The non-linear programming technique optimizes the values of the control parameters in order to enlarge the stability region of the system.
(5) Check the stability of the system through a time domain simulation with the inclusion of the worst contingency. This step is necessary since Eq. (12) only guarantees local stability. The time domain analysis check for global stability of the system with the parameter set obtained at step (4). If the system reaches a stable equilibrium point, go to step (6). Otherwise, go to step (3).
(6) End.

Fig. 1 depicts the flowchart of the proposed technique for large-disturbance stability control.

Observe that the algorithm performance depends on the value of Δ. If Δ is high, the algorithm solves Eq. (12) for a reduced number of times; however it is possible that the final result is too conservative. On the other hand, if Δ is small, the procedure can be time-consuming, though more precise results are achieved. Based on several test cases, $\Delta = k(\mu' - 1)$, where μ' is the value of the critical loading condition without contingencies and $k \in [0.01, 0.1]$ depending on the severity of the fault.

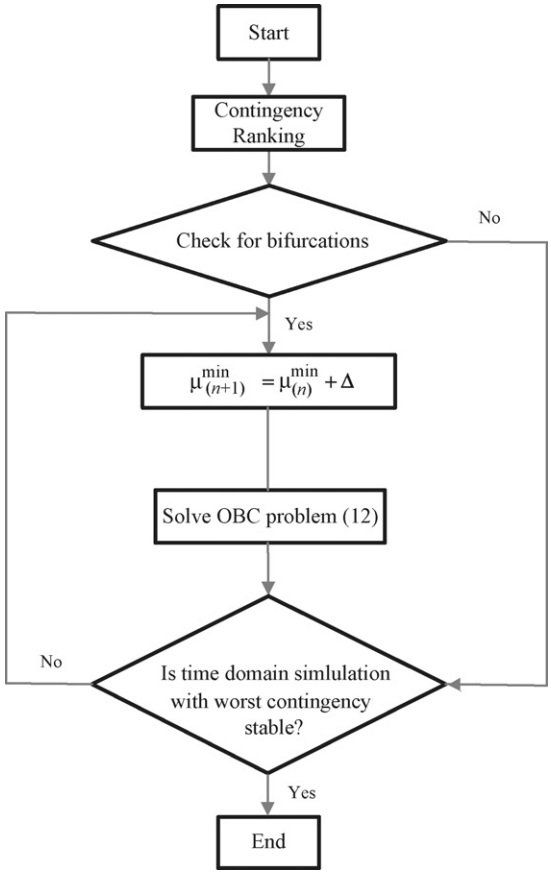

Fig. 1. Flow chart of the proposed optimal bifurcation control for improving post-disturbance stability.

Problem (12) is highly non-linear and can be badly conditioned at the bifurcation points. Thus the SQP method can fail to converge for large systems if it is not properly initialized. At this aim, if it is needed, we use a continuation method to determine a good initial guess. The continuation analysis allows getting a solution close to the bifurcation point of Eq. (12). The tangent vector of the state matrix is also a good initial guess for the eigenvectors u_x and u_y [30].

As a final remark, it has to be noted that determining the occurrence of an HB point is not trivial. Roughly speaking, if the system presents an undamped oscillations after the contingency, a Hopf bifurcation has likely occurred. However, an accurate bifurcation point tracing method is used in this paper to detect the occurrence of Hopf bifurcation points [11].

5. Cases studies

The proposed technique for large-disturbance stability control is applied to the WSCC 9-bus test system [31] and New England 39-bus test system [32]. The optimization problem (12) was solved using a sequential quadratic programming (SQP) algorithm, while time domain simulations and eigenvalue analyses were carried out using the Matlab-based toolbox PST [33]. Finally, for the interested reader, a detailed description of all static and dynamic models used in the case studies can be found in Ref. [33].

5.1. WSCC 9-bus test case

Fig. 2 depicts the WSCC 9-bus test system. All system data are depicted in Ref. [31], except for the gains of AVR, that are chosen as follows: $K_{A1} = K_{A2} = K_{A3} = 100$.

5.1.1. Optimal Hopf bifurcation control with V_{ref}

It is assumed that the current load level is 110% with respect to the data used in Ref. [31]. The loading margin that corresponds to this load profile is $\mu' = 1.32$. The worst case contingency is the line 7–8 outage, which leads to a Hopf bifurcation.

Table 1 depicts the objective function, the control variables, the inequality constraints and the step size Δ that are used to set up the OBC problem (12).

Table 2 illustrates the steps of the proposed OBC technique. The procedure ends in three steps for $\mu = 1.0192$. The results

Table 1
OBC settings for the WSCC test system with V_{ref} control

	AVR reference voltage $[V_{\text{ref1}}, V_{\text{ref2}}, V_{\text{ref3}}]$
Objective functions	$C(V_{\text{ref}}) = ((V_{\text{ref}} - V^0_{\text{ref}})^2)^{\text{T}} c_{V_{\text{ref}}}, \quad c_{V_{\text{ref}}} = [1, 1, 1]$
Inequality constraints, h	$0.95 \le V_i \le 1.15$ and regulator limits
Step size	$\Delta = 0.0064$

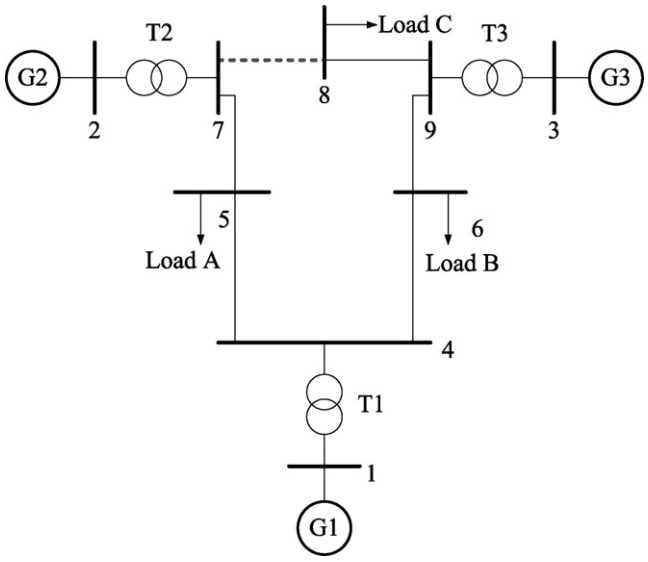

Fig. 2. WSCC 9-bus test system.

Table 2
Steps of the OBC technique for the WSCC 9-bus test system (variable V_{ref})

Variable	First step	Second step	Third step
μ	1.0064	1.0128	1.0192
V_{ref1}	1.0508	1.0508	1.0508
V_{ref2}	1.0445	1.0463	1.0485
V_{ref3}	1.0390	1.0390	1.0390

indicate that only the reference voltage of the generator 2 needs to be adjusted, as follows $V_{ref2} = 1.0485$.

Fig. 3 depicts the time domain simulation results for the line 7–8 outage without OBC ($V_{ref2} = 1.0429$) and with OBC ($V_{ref2} = 1.0485$), respectively. Observe that, without control, the system presents a frequency instability. Using the OBC, the system remains stable, though close to critical oscillations.

Table 3
OBC settings for the WSCC test system

	Gains of AVR [K_{A1}, K_{A2}, K_{A3}]
Objective functions	$C(K_A) = ((K_A - K_A^0)^2)^T c_{K_A}$, $c_{K_A} = [1, 1, 1]$
Inequality constraints, h	$0.95 \le V_i \le 1.15$ and regulator limits
Step size	$\Delta = 0.1 \times (1.346 - 1) = 0.0346$

Table 4
Steps of the OBC technique for the WSCC 9-bus test system (variable K_A)

Variable	First step	Second step	Third step	Fourth step
μ	1.0346	1.0692	1.1038	1.1384
K_{A1}	150	150	150	150
K_{A2}	161.8	176.47	191.62	207.4
K_{A3}	150	150	150	150

5.1.2. *Optimal Hopf bifurcation control with K_A*

In this case, we set the load level to 120% and all the AVR gains to 150. The loading margin that corresponds to the given load level is $\mu' = 1.346$. We use AVR gains as control variables. Table 3 illustrates the complete control information for the case study.

Table 4 illustrates the steps of the proposed OBC technique. The procedure ends in four steps for $\mu = 1.1384$. The results indicate that only the gain of AVR of the generator 2 needs to be adjusted, as follows $K_{A2} = 207.4$.

Fig. 4 depicts the time domain simulation results for the line 7–8 outage without OBC ($K_{A2} = 150$) and with OBC ($K_{A2} = 207.4$), respectively. Without control, the system presents a frequency instability, while using the OBC, the system remains stable.

It has to be noted that the main goal of this paper is to provide the "minimum" variation of control variables that lead to a stable system. The equilibrium point after the contingency is close to the bifurcation point, which results in a low-damped oscillation (see Figs. 3 and 4). The inclusion of new devices or controllers

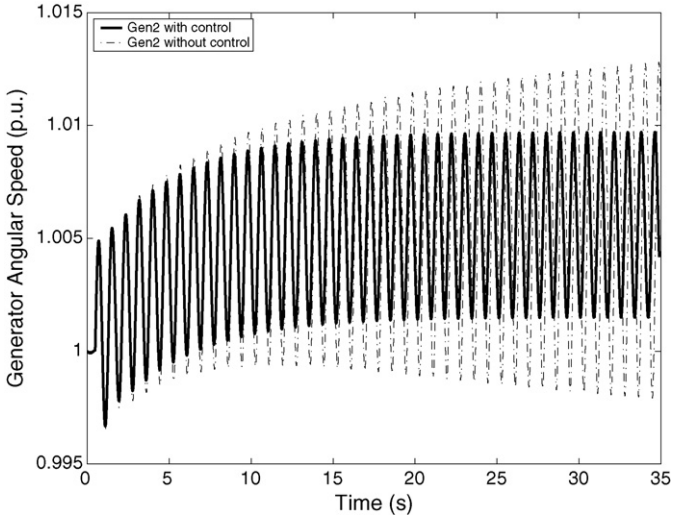

Fig. 3. Time domain simulation for the WSCC 9-bus test system with the line 7–8 outage, without control and with AVR reference voltage control ($V_{ref2} = 1.0485$).

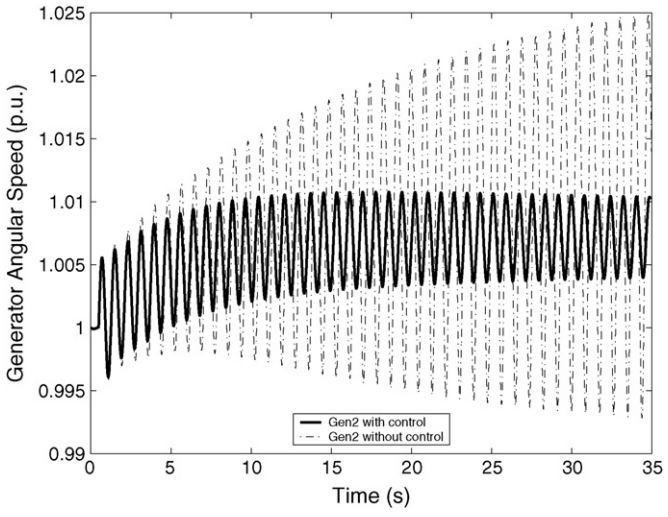

Fig. 4. Time domain simulation for the WSCC 9-bus test system with the line 7–8 outage, without control and with AVR gain control ($K_{A2} = 207.4$).

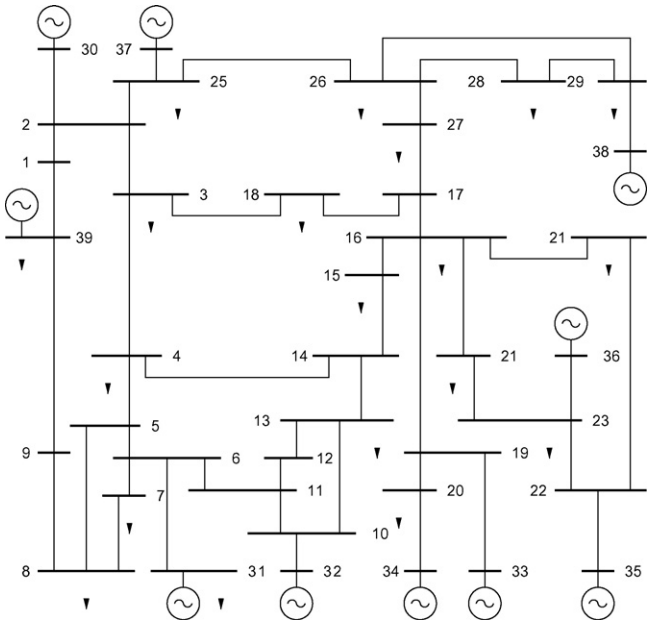

Fig. 5. New England 39-bus test system.

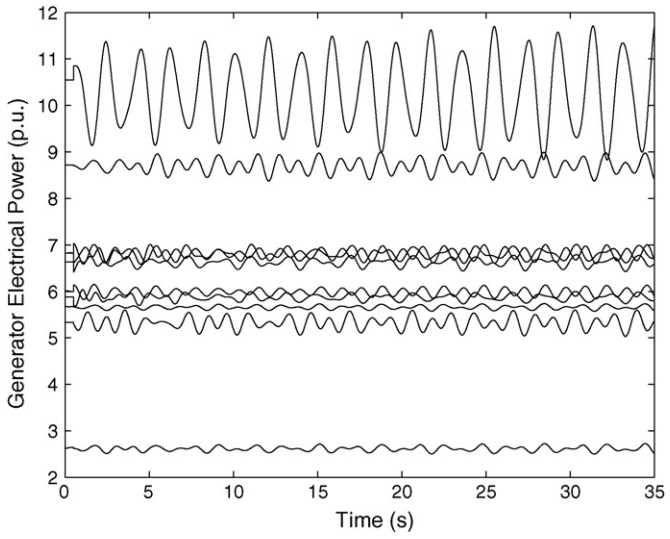

Fig. 6. Time domain simulation for the New England test system with the line 15–16 outage and without control.

such as PSS, could help in damping the oscillations. However, the design of this kind of corrective actions is beyond the scope of this paper.

The results of the WSCC system clearly indicate that AVR control gains are more effective than reference voltages for damping oscillations and avoiding the occurrence of Hopf bifurcations.

5.2. New England 39-bus test case

Fig. 5 depicts the New England 39-bus test system. Static and dynamic data of this case study can be found in Ref. [32].

5.2.1. Optimal Hopf bifurcation control with K_A

We set the current load level to 105%. The loading margin that corresponds to this load profile is $\mu' = 1.13$. The line 15–16 outage is the worst contingency and leads to a Hopf bifurcation. Thus the OBC technique is used to ensure the $N-1$ contingency stability of the system.

In this case, we use AVR gains K_A as controllable parameters. Furthermore, in order to reduce the computational burden, we select only a few AVR gains through a model analysis, as explained below.

In the New England test system, all generator damping torques are zero. Thus generator rotor speeds always present an undamped oscillation. However, this has not to be confused with Hopf bifurcations.

Fig. 6 depicts the time domain simulation results for the line 15–16 outage without control. The system shows an oscillatory instability triggered by a Hopf bifurcation. The frequency of the unstable oscillation is about 0.5 Hz. AVR gains K_{A5} and K_{A10} are selected as the strong-correlative control parameters because of the higher participation factor to the unstable complex eigenvalue pair. The OBC settings is the same as Table 3 except for the control parameters ($[K_{A5}, K_{A10}]$) and the step size ($\Delta = 0.05 \times (1.13 - 1) = 0.0065$).

For the solution of this test case, a continuation technique was used to get a good initial guess for Eq. (12). Simulation results show that the iterative process converges in a few iterations if using a good initial guess.

Table 5 reports the steps of the proposed OBC technique. The overall procedure ends in three steps for $\mu = 1.0195$. Furthermore, the results indicate that only the gain of the AVR of the generator 5 needs to be adjusted.

Fig. 7 depicts the time domain simulation results for the line 15–16 outage with OBC ($K_{A5} = 28.3$). Observe that, using the OBC, the system remains stable.

5.2.2. Optimal saddle-node bifurcation control with V_{ref}

For this case study, two banks of 50 MVAr capacitors are connected at buses 12 and 15, respectively. Loads at buses 4, 12 and 15 are modeled as induction motors, while a constant impedance model is used for the other load buses. It is assumed that the current load level is 114% with respect to the data used in Ref. [32]. The loading margin that corresponds to this load profile is $\mu' = 1.96$. The worst case contingency is the line 15–16 outage, which leads to a saddle-node bifurcation.

Table 6 depicts the objective function, the control variables, the inequality constraints and the step size Δ that are used to set up the OBC problem (12). In this case, defining a good initial guess is not an issue, since the size of Eq. (12) in the case of saddle-node bifurcation control is the half the size of Hopf

Table 5
Steps of the OBC technique for the New England test system (HB control)

Variable	First step	Second step	Third step
μ	1.0065	1.013	1.0195
K_{A5}	35.8	31.4	28.3
K_{A10}	40	40	40

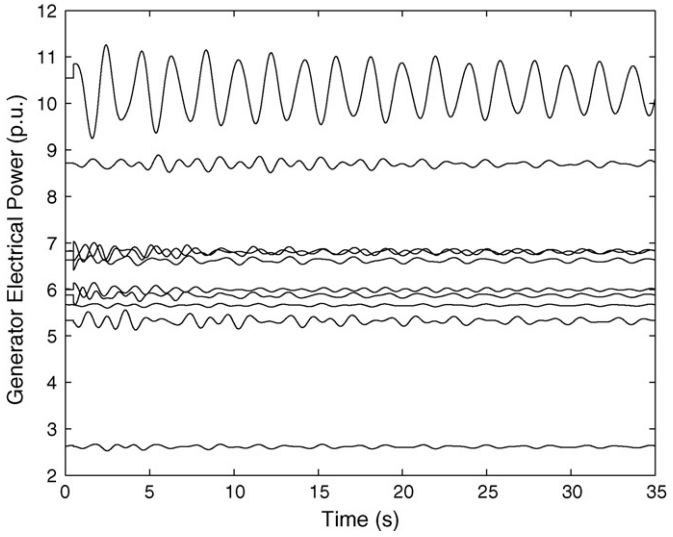

Fig. 7. Time domain simulation for the New England test system with the line 15–16 outage and with AVR gain control.

Table 6
OBC settings for the New England 39-bus test system

	AVR reference set-point, V_{ref}
Objective functions	$C(V_{ref}) = ((V_{ref} - V_{ref}^0)^2)^T c_{V_{ref}}, \quad c_{V_{ref}} = [1, 1, \ldots, 1]$
Inequality constraints	$0.95 \leq V_i \leq 1.15$ and regulator limits
Step size	$\Delta = 0.01$

bifurcation control. Thus, all AVR reference voltages V_{ref} can vary.

Table 7 illustrates the steps of the proposed OBC technique. The procedure ends in two steps for $\mu = 1.045$. The results indicate that only a few AVR reference voltages need to be adjusted.

Figs. 8 and 9 depict the time domain simulation results for the line 15–16 outage without and with OBC, respectively. Observe that, without control, the system presents a monotonic instability. Using the OBC, the system remains stable, though close to voltage stability limits. The inclusion of new devices or controllers such as SVC, could help in recovering the voltage profile. However, the design of this kind of corrective actions is beyond the scope of this paper.

Table 7
Steps of the OBC technique for the New England 39-bus test system (SNB control)

Bus number	AVR reference voltage, V_{ref}	
	Pre-optimization ($\mu = 1.025$)	Post-optimization ($\mu = 1.045$)
30	1.2451	1.2451
31	1.3720	1.3720
32	1.3338	1.4038
33	1.3429	1.4451
34	1.6703	1.7534
35	1.4137	1.4137
36	1.4027	1.4027
37	1.3316	1.3316
38	1.3754	1.3838
39	1.2060	1.2060

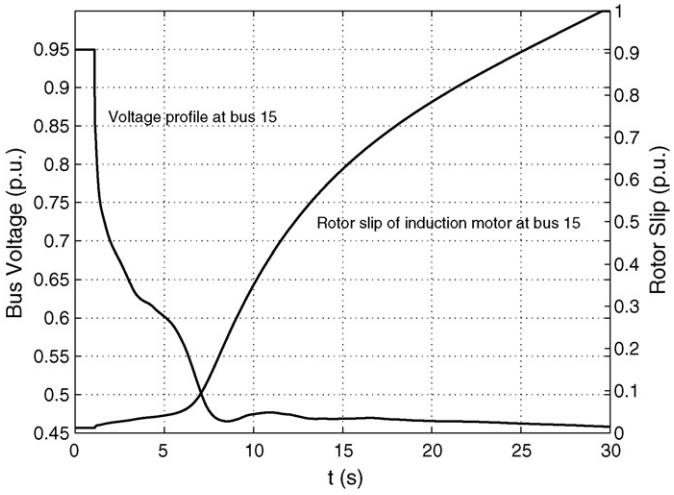

Fig. 8. Time domain simulation for the New England 39-bus test system with the line 15–16 outage and without control.

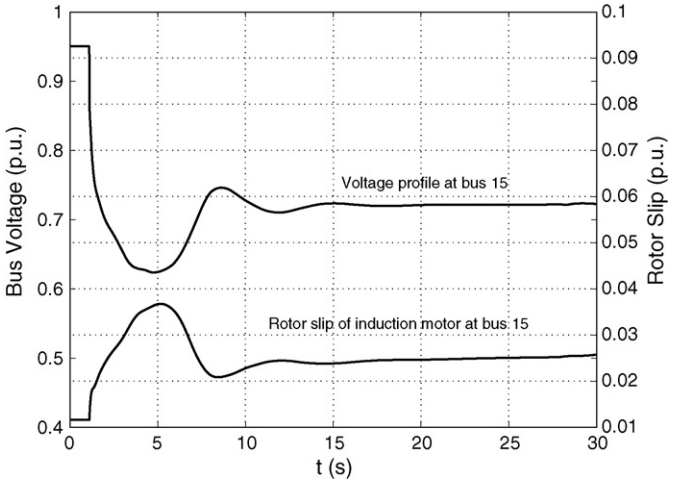

Fig. 9. Time domain simulation for the New England 39-bus test system with the line 15–16 outage and with AVR voltage reference control.

As a final remark, observe that the AVR references are effective parameters for saddle-node bifurcation control, as expected, since increasing generator voltages allows increasing the network loadability [30].

6. Conclusion

A novel approach for large-disturbance stability control is proposed and discussed in this paper. The proposed optimal bifurcation control addresses in particular saddle-node and Hopf bifurcations and is tested through two benchmark case studies.

The advantages of the proposed method are as follows:

(1) It provides an approximate loading margin that is a measure of system stability.
(2) It works for both saddle-node and Hopf bifurcations, i.e. for voltage and frequency instability.

(3) The use of time domain simulations also allows excluding the occurrence of transient instabilities and avoid bifurcations triggered by contingencies.

Future works will concentrate on finding a simple criterion to find adequate values for the step increment Δ, whose evaluation is currently based on off-line analyses. The authors are currently testing the proposed method on large-scale case studies.

Acknowledgments

Federico Milano is partly supported by the Ministry of Science and Education of Spain through CICYT Project DPI-2003-01362 and by Junta de Comunidades de Castilla-La Mancha through project PBI-05-053.

References

[1] M.A. Pai, Energy Function Analysis for Power System Stability, Kluwer Academic Publishers, Norwell, 1989.
[2] Y. Ni, S. Chen, B. Zhang, Theory and Analysis of Dynamic Power Systems, Tsinghua University Press, Beijing, 2002.
[3] H.-D. Chiang, C.-C. Chu, G. Cauley, Direct stability analysis of electric power systems using energy functions: theory, applications, and perspective, Proc. IEEE 83 (11) (1995) 1497–1529.
[4] V. Vittal, Consequence and impact of electric utility industry restructuring on transient stability and small-signal stability analysis, Proc. IEEE 88 (2) (2000) 196–207.
[5] Y. Xue, Extended equal area criterion revised, IEEE Trans. Power Syst. 7 (1992) 1012–1022.
[6] M. Ilić, J. Zaborszky, Dynamic Control of Large Electric Power Systems, Wiley-Interscience Publication, New York, 2000.
[7] T. Van Cutsem, M.E. Grenier, D. Lefebvre, Combined detailed and quasi steady-state time simulations for large-disturbance analysis, Int. J. Elect. Power Energy Syst. 28 (9) (2006) 634–642.
[8] C.D. Vournas, N.G. Sakellaridis, Region of attraction in a power system with discrete LTCs, IEEE Trans. Power Syst. 53 (7) (2006) 1610–1618.
[9] D. Ruiz-Vega, M. Pavella, A comprehensive approach to transient stability control. I. Near optimal preventive control, IEEE Trans. Power Syst. 18 (4) (2003) 1446–1453.
[10] D. Ruiz-Vega, M. Pavella, A comprehensive approach to transient stability control. II. Open loop emergency control, IEEE Trans. Power Syst. 18 (4) (2003) 1446–1453.
[11] R. Seydel, Practical Bifurcation and Stability Analysis: from Equilibrium to Chaos, 2nd ed., Springer-Verlag, New York, 1994.
[12] V. Venkatasubramanian, H. Schattler, J. Zaborszky, Dynamics of large constrained nonlinear systems—a taxonomy theory, Proc. IEEE 83 (11) (1995) 1530–1561.
[13] V. Venkatasubramanian, H. Schattler, J. Zaborszky, Local bifurcations and feasibility regions in differential-algebraic systems, IEEE Trans. Automat. Control 40 (12) (1995) 1992–2013.
[14] W. Rosehart, C.A. Cañnizares, V.H. Quintana, Optimal power flow incorporating voltage collapse constraints, in: Proceedings of the 1999 IEEE-PES Summer Meeting, Edmonton, Alberta, 1999, pp. 820–825.
[15] C.A. Cañizares, W. Rosehart, A. Berizzi, C. Bovo, Comparison of voltage security constrained optimal power flow techniques, in: Proceedings of the 2001 IEEE-PES Summer Meeting, Vancouver, BC, Canada, 2001, pp. 1680–1685.
[16] W.D. Rosehart, C.A. Cañizares, V. Quintana, Multi-objective optimal power flows to evaluate voltage security costs in power networks, IEEE Trans. Power Syst. 18 (2) (2003) 578–587.
[17] F. Milano, C.A. Cañizares, M. Invernizzi, Voltage stability constrained OPF market models considering $N-1$ contingency criteria, Elect. Power Syst. Res. 74 (1) (2005) 27–36.
[18] C.A. Cañizares, Calculating optimal system parameters to maximize the distance to saddle-node bifurcations, IEEE Trans. Circuits Syst.-I. Fundam. Theory Appl. 45 (3) (1998) 225–237.
[19] M.M. Begović, G. Phadke, Control of voltage stability using sensitivity analysis, IEEE Trans. Power Syst. 7 (1) (1992) 114–120.
[20] S. Greene, I. Dobson, F.L. Alvarado, Contingency ranking for voltage collapse via sensitivities from single nose curve, IEEE Trans. Power Syst. 14 (1) (1999) 232–240.
[21] F. Capitanescu, T. Van Cutsem, Unified sensitivity analysis of unstable or low voltages caused by load increases or contingencys, IEEE Trans. Power Syst. 20 (1) (2005) 321–329.
[22] S. Greene, I. Dobson, F.L. Alvarado, Sensitivity of transfer capability margins with a fast formula, IEEE Trans. Power Syst. 17 (1) (2002) 34–40.
[23] C.A. Cañizares, C. Cavallo, M. Pozzi, S. Corsi, Comparing secondary voltage regulation and shunt compensation for improving voltage stability and transfer capability in the Italian power system, Elect. Power Syst. Res. 73 (1) (2005) 67–76.
[24] S. Wunderlich, T. Wu, R. Fischl, R. O'Connell, An inter-area transmission and voltage limitation (TVLIM) program, IEEE Trans. Power Syst. 10 (3) (1995) 1257–1263.
[25] N. Mithulananthan, C.A. Cañizares, J. Reeve, J.J. Rogers, Comparison of PSS, SVC, and STATCOM controllers for damping power system oscillations, IEEE Trans. Power Syst. 18 (2) (2003) 786–792.
[26] C.A. Cañizares, N. Mithulananthan, F. Milano, J. Reeve, Linear performance indices to predict oscillatory stability problems in power systems, IEEE Trans. Power Syst. 19 (2) (2004) 1104–1114.
[27] T. Van Cutsem, An approach to corrective control of voltage instability using simulation and sensitivity, IEEE Trans. Power Syst. 10 (2) (1995) 616–622.
[28] T. Van Cutsem, C. Vournas, Voltage stability analysis in transient and mid-term time scales, IEEE Trans. Power Syst. 11 (1) (1996) 146–154.
[29] P. Kundur, Power System Stability and Control, McGraw Hill, New York, 1994.
[30] C.A. Cañizares, Voltage stability assessment: concepts, practices and tools, Tech. rep., IEEE/PES Power System Stability Subcommittee, Final Document, August 2002.
[31] P.W. Sauer, M.A. Pai, Power System Dynamics and Stability, Prentice Hall, Upper Saddle River, NJ, 1998.
[32] W. Gu, Optimal bifurcation control in power systems, PhD Thesis, Southeast University, China, May 2006.
[33] Cherry Tree Scientific Software, Power System Toolbox Ver. 2.0: Dynamic Tutorial and Functions, 1999.